RSC Advances

PAPER

View Article Online
View Journal | View Issue



Cite this: *RSC Adv.*, 2023, **13**, 22831

# Preparation and characterization of PA/P(AA-*co*-AM) composite hydrogels *via* photopolymerization

Bin Li, * Wenrui Hao, Aolin Wu, Mengjing Zhou, Qinghua Yan, Heng Zhang and Lihua Su

Received 20th June 2023
Accepted 20th July 2023

DOI: 10.1039/d3ra04118b

rsc.li/rsc-advances

The present study synthesized a deep eutectic solvent (DES) using acrylic acid (AA), acrylamide (AM), and choline chloride (ChCl), and added phytic acid (PA) as a filler. Subsequently, the PA/P(AA-*co*-AM) composite hydrogel was prepared under ultraviolet irradiation and used a photoinitiator. Characterization of the hydrogels was conducted using Fourier transform infrared spectroscopy (FTIR) and scanning electron microscopy (SEM). The study aimed to investigate the impact of PA on the mechanical properties, fatigue resistance, and electrical conductivity of the composite hydrogel. The findings demonstrated that as the mass fraction of PA increased, the compressive strength of the composite hydrogel gradually decreased, yet the fatigue resistance of the composite hydrogel increased. Specifically, after 10 cycles of compression, the resilience recovery rate of FP0 dropped from 86.9% to 70.4%, the maximum stress recovery rate of FP1 dropped from 97.9% to 89.4%, the maximum stress recovery rate of FP2 dropped from 94.4% to 86.6%, and the maximum stress recovery rate of FP3 dropped from 97.3% to 93%. Overall, this study offers a straightforward and efficient method for producing composite hydrogels with both fatigue resistance and electrical conductivity.



## 1 Introduction

Hydrogels are polymers with a unique three-dimensional network structure that maintain their insolubility while absorbing a considerable amount of water.[1–3] Due to their excellent water-holding and moisturizing properties, hydrogels have been widely used in various fields such as agriculture, medicine, and environmental protection. In the agricultural sector, hydrogels can be added to soil to increase soil water retention and improve the water utilization efficiency in plant growth.[4] In the medical field, hydrogels can be used as a drug carrier to deliver drugs to specific locations in the human body, improving drug safety and efficacy.[5–7] In the field of environmental protection, hydrogels can be used to absorb organic matter and heavy metal ions in wastewater, improving water quality.[8,9] However, the widespread application of most hydrogels is seriously limited due to their poor fatigue resistance and conductivity. Therefore, hydrogels with good fatigue resistance and conductivity are more advantageous in practical applications.[10]

Phytic acid (PA), also known as inositol hexaphosphate, is found in most grains, legumes, and nuts.[11,12] As a green and environmentally friendly biomass material, PA has been extensively used in fields such as food, materials, and pharmaceuticals.[13] PA contains a large number of hydroxyl and phosphate groups in its structure, which can ionize hydrogen ions ($H^+$). Moreover, PA has characteristics of non-toxicity, low cost, easy accessibility, and environmental friendliness.[14] Furthermore, inspired by the strong chelation interactions of many biomass materials, PA has been used as an ideal cross-linking agent for hydrogels.[15]

Deep eutectic solvents (DES) are a new type of almost non-toxic and green reagents composed of a mixture of hydrogen bond acceptors (HBA) and hydrogen bond donors (HBD), with properties such as low toxicity, low cost, biodegradability, and environmental friendliness.[19] One of the common DES is composed of choline chloride (ChCl) as HBA and other HBDs.[20] Due to the rich hydrogen bond network formed by the interaction between ChCl and HBD, the melting point of the resulting mixture is much lower than that of individual components. One of the common DES is composed of choline chloride (ChCl) as HBA and other HBDs.[20] Due to the rich hydrogen bond network formed by the interaction between ChCl and HBD, the melting point of the resulting mixture is much lower than that of individual components.[21] When DES is used for photopolymerization reactions, it can act as both a monomer or a medium and provide a high viscosity environment to suppress buoyancy-driven convection without the need for additional materials.

Photopolymerization is a novel polymerization method that does not require the use of initiators commonly used in traditional polymerization, avoiding issues of initiator residue and the impact of initiators on polymer properties.[16] Moreover,

*School of Mechanical Engineering, Wuhan Polytechnic University, Wuhan, Hubei 430023, China. E-mail: lb420@whpu.edu.cn*

photopolymerization can be conducted at room temperature without the need for high temperature and pressure conditions, with simple and convenient operation, fast reaction rate, short reaction time, and greatly improved production efficiency.[17] Finally, photopolymerization is an environmentally friendly and low-energy polymerization method that meets the requirements of sustainable development.[18]

Based on previous research, we added phytic acid (PA) to DES and developed an anti-fatigue PA/P(AA-*co*-AM) composite hydrogel. PA/P(AA-*co*-M) composite hydrogels were successfully synthesized by mixing AA, AM, and ChCl in a molar ratio of 1.5 : 0.5 : 1 and adding varying amounts of PA to DES for polymerization. The structure of the composite hydrogel was characterized by scanning electron microscopy (SEM) and Fourier transform infrared spectroscopy (FTIR). The performance of the composite hydrogel was tested, and the effects of different PA contents on the pH responsiveness, anti-fatigue properties, and conductivity of the composite hydrogel were further analysed.

# 2 Materials and methods

## 2.1 Materials

Phytic acid (PA, 50 wt% aqueous solution, relative molecular mass of 660.04), choline chloride (ChCl), acrylic acid (AA), acrylamide (AM), and crosslinking agent *N*,*N*-methylenebisacrylamide (MBA) were all purchased from Aladdin Chemistry Co., Ltd in Shanghai, China. All of the above chemicals were of analytical grade and could be used directly. Prior to use, ChCl was dried in a vacuum drying oven at 70 °C for two hours to remove any water. Deionized water was used for all experiments.

## 2.2 Preparation of DES

ChCl was used as the HBA, while AA and AM were used as HBD. The three raw materials were mixed in a molar ratio of 1 : 1.5 : 0.5 and placed in a beaker, which was then immersed in a 70 °C oil bath and continuously stirred until a transparent and clear liquid, *i.e.*, DES, was formed, as shown in Fig. 1(a). The hydrogen bond structure of DES is shown in Fig. 1(c).

## 2.3 Photo-polymerization preparation of PA/P(AA-*co*-AM) composite hydrogel

At room temperature of 25 °C, the filler phytic acid (PA), crosslinker *N*,*N*′-methylenebisacrylamide (MBA), and photoinitiator were successively added to the DES according to the proportion specified in Table 1. The mixture was stirred until homogeneous, then poured into a test tube (100 mm in length and 12 mm in diameter), and exposed to UV light at a wavelength of 365 nm. After the solution was gelled, the test tube was inverted, and if the gel did not flow and could be maintained for more than 10 seconds, the transition from liquid to gel had occurred. Finally, after the test tube temperature cooled to room temperature, the prepared hydrogel sample was taken out from the test tube for future use. The preparation process of the composite hydrogel is shown in Fig. 2.

## 2.4 Characterization of PA/P(AA-*co*-AM) composite hydrogels

The polymer was first cut into 1 mm-thick circular discs, soaked in distilled water for 7 days to remove the water-soluble ChCl, and then the cylindrical hydrogel samples were pre-frozen in a freezer and subsequently freeze-dried in a cold vacuum dryer at −60 °C for 2 days until constant weight was reached. The dried hydrogel sample was ground into powder, mixed with potassium bromide, ground and pressed into pellets, and analyzed for its spectral characteristics using Fourier transform infrared spectrometer (FTIR). The vacuum freeze-dried samples were coated with gold using a high vacuum ion sputtering

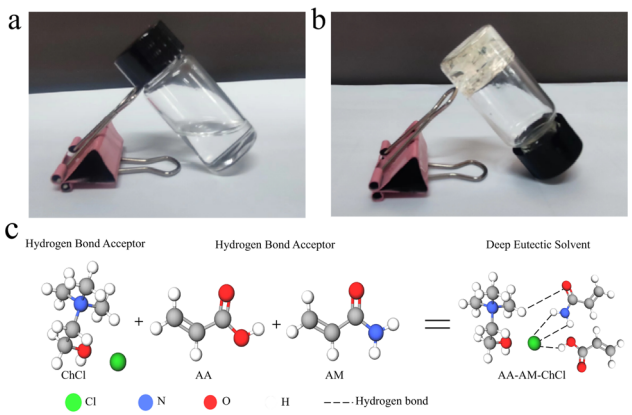


Fig. 1 (a) Photograph of DES before photo-polymerization. (b) Photograph of DES after photo-polymerization. (c) Hydrogen bond structure diagram of DES.

Table 1 Composition and proportion of DES

| Sample | AA/AM/ChCl (molar ratio) | PA (wt%) | MBA (wt%) |
|---|---|---|---|
| FP0 | 1.5 : 0.5 : 1 | 0 | 1 |
| FP1 | 1.5 : 0.5 : 1 | 0.2 | 1 |
| FP2 | 1.5 : 0.5 : 1 | 0.4 | 1 |
| FP3 | 1.5 : 0.5 : 1 | 0.5 | 1 |

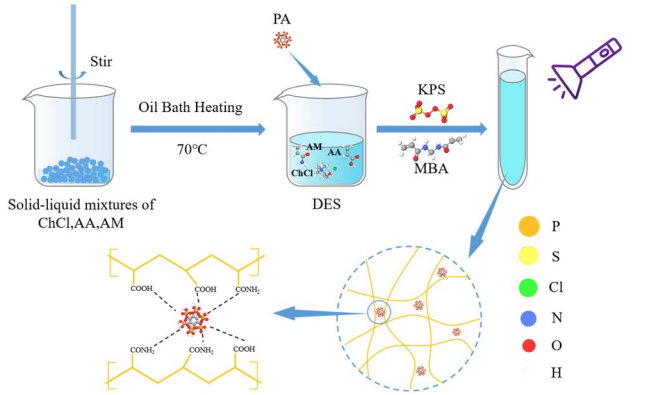


Fig. 2 Schematic diagram of preparation of composite hydrogel.

instrument for cross-sectional observation of the microstructure using SEM.

### 2.5 Performance test of 2.5 PA/P(AA-*co*-AM) composite hydrogel

**2.5.1 Hydrogel mechanical properties test.** The compressive properties of the composite hydrogel were tested using a Shanghai Bose TA.XTC-18 mass spectrometer, with the compression head compressed at a rate of 10 mm $min^{-1}$ until the maximum compressive stress was obtained. The formula (1) for calculating the compressive strength is as follows:

$$P = \frac{F}{S} \quad (1)$$

In formula (1), $F$ is the applied force, and $S$ is the cross-sectional area of the hydrogel.

**2.5.2 Testing of the fatigue resistance of the hydrogel.** The fatigue resistance of the hydrogel was characterized in 10 cyclic compression tests with a strain of 80% and no rest time, and the formula (2) for the toughness recovery rate is as follows:

$$R = \frac{S_{ci}}{S_{c1}} \quad (2)$$

In formula (2), $S_{ci}$ represents the integral area of the hysteresis loop during the $i$-th cycle of cyclic compression of the hydrogel, and $S_{c1}$ represents the integral area of the hysteresis loop during the first cycle of compression and recovery during stretching of the hydrogel.

The formula (3) for calculating the maximum stress recovery rate is as follows:

$$\eta = \frac{\sigma_i}{\sigma_1} \quad (3)$$

In formula (3), $\sigma_i$ represents the maximum stress during the $i$-th cycle of cyclic compression of the hydrogel, and $\sigma_1$ represents the maximum stress during the first cycle of cyclic compression of the hydrogel.

**2.5.3 Testing of the electrical conductivity of the hydrogel.** The resistance of cylindrical hydrogel samples was measured using a multimeter, and the formula for calculating the ionic conductivity is as follows:

$$\sigma = \frac{1}{R}\frac{d}{S} \quad (4)$$

In formula (4), the Greek letter $\sigma$ is used to represent the conductivity, with units of mS $cm^{-1}$; $d$ is the thickness of the hydrogel, with units of cm; $S$ is the cross-sectional area of the hydrogel, with units of $cm^2$; $R$ is the measured resistance, with units of Ω.

## 3 Results and discussion

### 3.1 Microscopic morphology analysis of PA/P(AA-*co*-AM) composite hydrogels

To investigate the effect of different contents of PA on the microstructure of P(AA-*co*-AM) hydrogels, the hydrogels were characterized by SEM, and Fig. 3 shows the SEM images of FP0–FP3 hydrogels at 200 times magnification. The hydrogels with

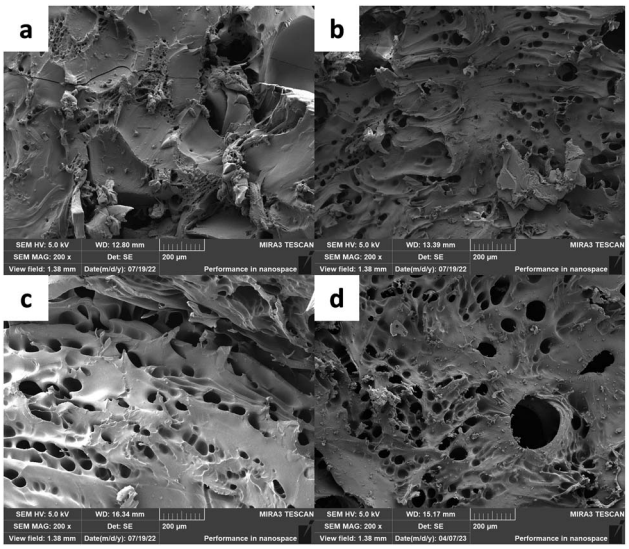


Fig. 3 SEM images of (a) FP0, (b) FP1, (c) FP2, (d) FP3 hydrogels.

different PA contents were placed in deionized water for 7 days to remove soluble substances such as choline chloride. After pre-freezing, the hydrogels were dried in a vacuum freeze dryer at −60 °C for 48 hours to obtain the freeze-dried composite hydrogels. It can be seen from the figure that the average pore size of PA/P(AA-*co*-AM) hydrogels increases with the increase of PA content, because PA has a high hydrophilicity and can absorb more water than samples without PA.[13] In addition, the size and morphology of the micropores become irregular and disordered with the increase of PA content. Compared with the no obvious pores in FP0 hydrogel, FP3 hydrogel exhibits an irregular honeycomb-like pore structure (as shown in Fig. 3(d)), which may be due to the hydrogen bonding between PA and the polymer network in P(AA-*co*-AM) hydrogel.[22,23]

### 3.2 Fourier infrared spectroscopy

Fig. 4 shows the FTIR spectra of PA, P(AA-*co*-AM) and PA/P(AA-*co*-AM) composite hydrogels containing 0.5 wt% PA. The absorption peak around 1639 $cm^{-1}$ for PA is related to the stretching vibration of O–P–O, and the small absorption peak at 1130 $cm^{-1}$ is attributed to the stretching vibration of P═O. The stretching vibration of $(PO_3)^{2-}$ causes an absorption peak at 1058 $cm^{-1}$. Meanwhile, a small absorption peak also appears near 950 $cm^{-1}$ in the spectrum of PA/P(AA-*co*-AM), which is related to the stretching vibration of $(PO_3)^{2-}$.[24] In the spectrum of the P(AA-*co*-AM) hydrogel, the stretching vibrations of the N–H group on the AM unit and the OH group on the AA unit overlap, forming a broad absorption peak at 3442 $cm^{-1}$.[25] Compared with the spectrum of P(AA-*co*-AM) hydrogel, the stretching vibration of the C═O group on the PA/P(AA-*co*-AM) hydrogel is shifted from 1722 $cm^{-1}$ to 1733 $cm^{-1}$, and the asymmetric stretching of the COO– group is shifted from 1639 $cm^{-1}$ to 1654 $cm^{-1}$. In the spectrum of the PA/P(AA-*co*-AM) hydrogel, the absorption intensity of the C═O group and the COO– group is increased.[26–28] The stretching vibration of C–N in the $CO{=}NH_2$ unit results in an absorption peak at 1454 $cm^{-1}$,

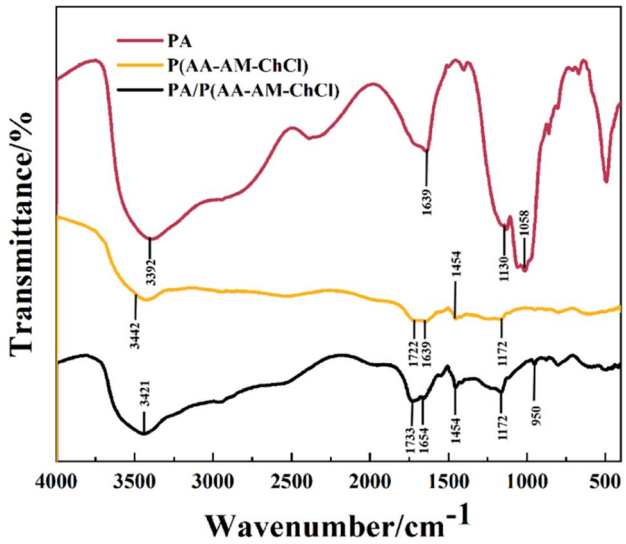


Fig. 4 Shows the FTIR spectra of PA, P(AA-*co*-AM), and PA/P(AA-*co*-AM) hydrogels.

and the stretching vibration of C–O in the COOH unit results in an absorption peak at 1172 $cm^{-1}$.[25] However, the absorption peaks at 1454 $cm^{-1}$ and 1172 $cm^{-1}$ are enhanced in the spectrum of the PA/P(AA-*co*-AM) hydrogel.

### 3.3 Compression and fatigue resistance of PA/P(AA-*co*-AM) composite hydrogel

We conducted compression tests and analysis on phytic acid hydrogels with different mass fractions, and some of the experimental processes are shown in Fig. 5(a). The maximum compressive strengths of FP0, FP1, FP2, and FP3 hydrogels were 0.95 MPa, 0.61 MPa, 0.47 MPa, and 0.41 MPa, respectively. The compressive strength of the composite hydrogel gradually decreased with the increase of PA content, which was attributed to the addition of phytic acid solution and the introduction of water, making the molecular chains more prone to slip under stress, thereby reducing the compressive strength of the material.[29] Fig. 5(d) and (e) show the 10-cycle compression curves of FP0 and FP2 hydrogels at 80% strain, and the curves of the maximum stress of FP0 and FP2 hydrogels over time are also displayed. From the 5th to the 10th cycle of compression, the curve of the maximum stress of FP2 hydrogel with respect to time was smoother compared to that of FP0 hydrogel.[30] After 10 cycles of compression, the toughness recovery rate of FP0 hydrogel decreased from 86.9% to 70.4%, and the maximum stress recovery rate decreased from 97.9% to 89.4%; the toughness recovery rate of FP2 hydrogel decreased from 94.4% to 86.6%, and the maximum stress recovery rate decreased from 97.3% to 93%, as shown in Fig. 5(c), indicating that the hydrogel with added PA has excellent anti-fatigue performance.

### 3.4 Conductivity of PA/P(AA-*co*-AM) composite hydrogel

In order to investigate the effect of different contents of PA on the electrical conductivity of the composite hydrogel, the

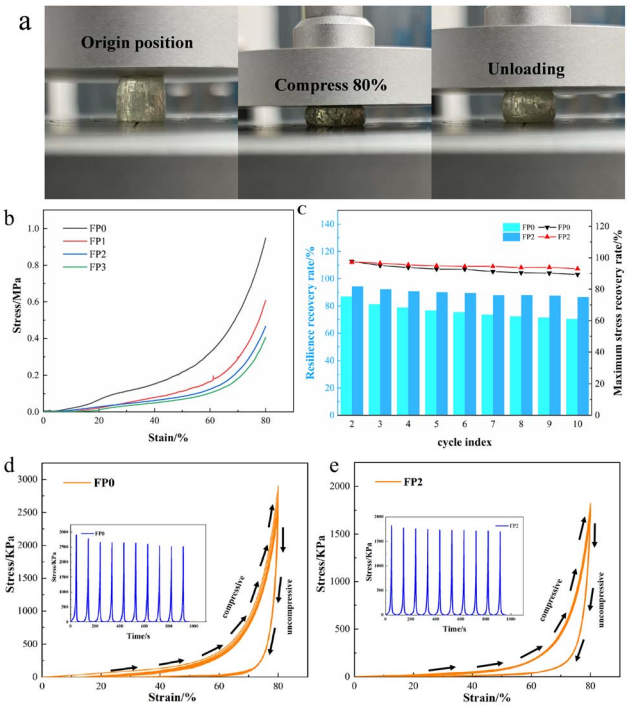


Fig. 5 (a) Demonstration of one loading–unloading cycle under 80% compressive strain deformation for hydrogels. (b) Compressive stress–strain curves of FP0, FP1, FP2, and FP3. (c) Toughness recovery rate and maximum stress recovery rate of FP0 and FP2 hydrogels after ten consecutive compression-unloading cycles. (d) and (e) Ten compression cycles stress–strain curves of FP0 and FP2 hydrogels under 80% strain.

conductivity of the samples was recorded at different time periods and temperatures. Fig. 6(a) shows the changes in conductivity of 4 groups of samples within 12 hours. It can be seen that with the increase of PA mass fraction, the conductivity of the composite hydrogel gradually increases. The conductivity of FP0, FP1, FP2 and FP3 at 12 h were 0.00326 mS $cm^{-1}$, 0.00472 mS $cm^{-1}$, 0.00979 mS $cm^{-1}$ and 0.0153 mS $cm^{-1}$, respectively. The conductivity of FP1, FP2 and FP3 (compared with FP0) increased by 1.4, 3.0 and 4.7 times, respectively. This is due to the good water absorption of ChCl in the hydrogel, which can absorb water molecules in the air. The water molecules entering the gel network promote the movement of chloride ions in the network, thus causing the change of conductivity.[31] In addition,

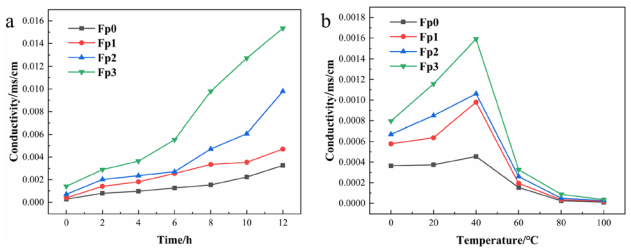


Fig. 6 (a) The conductivity of FP0, FP1, FP2, and FP3 hydrogels at different times. (b) The conductivity of FP0, FP1, FP2, and FP3 hydrogels at different temperatures.

after adding phytic acid solution, the concentration of free ions in the gel increased, including chloride ions and newly added hydrogen ions. In addition, phytic acid solution contains water molecules, and some water molecules will enter the interior of the gel, resulting in an increase in the conductivity of the gel. It should be noted, therefore, the conductivity of the composite hydrogel increases with the increase of PA content.[32]

Fig. 6(b) shows the conductivity of the composite hydrogel at different temperatures. The conductivity of 4 groups of hydrogels gradually increased in the range of 0–40 °C and gradually decreased in the range of 40–100 °C. This is because the temperature rise in the range of 0–40 °C can accelerate the movement of $H_3O^+$ as a proton carrier and activate the hydrogen bond network.[33] When the temperature rises from 40 °C to 100 °C, the water stored in the hydrogel gradually loses, which restricts the proton conduction group and proton migration rate, thus reducing the conductivity.[34]

### 3.5 pH response performance of 3.5 PA/P(AA-*co*-AM) composite hydrogels

Fig. 7 shows the swelling behavior of hydrogels with different PA contents at different pH values. At pH 3, the carboxylic acid molecules on PA and polymer chains become protonated. Due to the hydrogen bonding interaction between PA and –COOH on polymer chains, the polymer chains inside the composite hydrogel are intertwined and contracted, resulting in a lower ESR of the composite hydrogel.[1,35] When the pH increases to 4.8, –COOH on PA and polymer chains are converted into negatively charged –COO– ions. The weakening of hydrogen bonding between –COOH groups and the enhancement of electrostatic repulsion between –COO– ions lead to an increase in the swelling ratio of the composite hydrogel.[36] When the pH reaches 7, the hydrogen bonding between most non-ionized –COOH and $–CONH_2$ reduces the number of hydrophilic groups and makes the polymer network structure less prone to swell, resulting in a decrease in the swelling ratio of the composite hydrogel.[37] As the pH gradually increases to 9.4, the hydrogen bonds inside the hydrogel break, and the electrostatic repulsion between –COO– groups causes the polymer network space to expand, resulting in an increase in the swelling ratio of the hydrogel.[38] When the pH reaches 9.4, the swelling ratio of the hydrogel gradually decreases because $Na^+$ ions aggregate near the –COO– groups on PA and polymer chains due to the Coulomb effect, which weakens the electrostatic repulsion of the polymer and reduces the swelling ratio of the hydrogel.[39] At the same pH value, the swelling ratio of the hydrogel increases with the increase of PA content, which is because the hydrogel with higher PA content has more hydrophilic groups.[27]

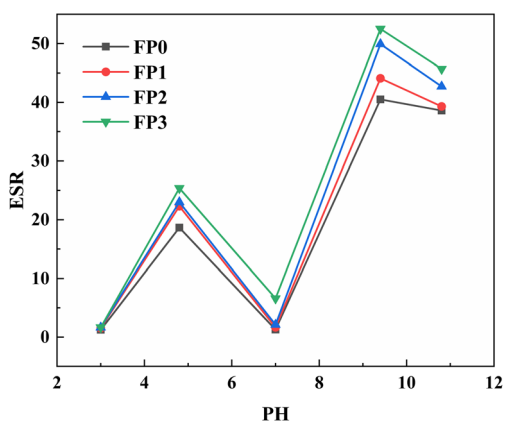


Fig. 7 Shows the pH response curve of PA/P(AA-*co*-AM) composite hydrogel.

## 4 Conclusions

This article added PA as a filler to the DES prepared with AA, AM, and ChCl as raw materials, and MBA as a crosslinking agent. A fatigue-resistant PA/P(AA-*co*-AM) composite hydrogel was successfully prepared by photopolymerization, and the structure and properties of the composite hydrogel were studied. The experimental results show that:

(1) Compression experiments showed that the compressive strength of the composite hydrogel decreased with the increase of PA content, which was due to the internal stress caused by PA aggregation and copolymerization network. Fatigue resistance tests showed that the higher the PA content in the composite hydrogel, the stronger the fatigue resistance. The toughness recovery rate of FP2 decreased from 94.4% to 86.6%, and the maximum stress recovery rate decreased from 97.3% to 93%.

(2) After adding PA, the conductivity of the composite hydrogel was significantly enhanced. The conductivity of the composite hydrogel with a PA content of 0.5% was 0.0153 mS $cm^{-1}$, which was 4.7 times higher than that of the hydrogel without PA. It can be used in electronic sensors and other fields.

(3) The PA/P(AA-*co*-AM) composite hydrogel has good pH responsiveness. With the change of pH, the swelling performance of the composite hydrogel shows a significant change, which makes the composite hydrogel have a good application prospect in sewage treatment.

## Author contributions

B. L., proposed the ideas, steps and details of the experiment, most of the experiments were done by W. R. H., M. J. Z., A. L. W., where W. R. H. was instrumental in the proper conduct of the experiments and wrote the article together with B. L., and all the authors analyzed the data, discussed the conclusions.

## Conflicts of interest

The authors declare that there are no competing interests regarding the publication of this article.

## Acknowledgements

The work is supported by 2022 Knowledge Innovation Dawn Special Plan Project (2022010801020393), Natural Science Foundation of Hubei Province (2021CFB292) and Research and Innovation Initiatives of WHPU (2022J04). This work was finished at Wuhan Polytechnic University, Wuhan.

## References

1 B. Li, X. Xu, Z. Hu, Y. Li, M. Zhou, J. Liu, Y. Jiang and P. Wang, Rapid preparation of N-CNTs/P(AA-co-AM) composite hydrogel via frontal polymerization and its mechanical and conductive properties, *RSC Adv.*, 2022, **12**, 19022–19028.

2 E. G. Arafa, M. W. Sabaa, R. R. Mohamed, E. M. Kamel, A. M. Elzanaty, A. M. Mahmoud and O. F. Abdel-Gawad, Eco-friendly and biodegradable sodium alginate/quaternized chitosan hydrogel for controlled release of urea and its antimicrobial activity, *Carbohydr. Polym.*, 2022, **291**, 119555.

3 Z. Zhang, T. Lin, S. Li, X. Chen, X. Que, L. Sheng, Y. Hu, J. Peng, H. Ma, J. Li, W. Zhang and M. Zhai, Polyacrylamide/Copper-Alginate Double Network Hydrogel Electrolyte with Excellent Mechanical Properties and Strain-Sensitivity, *Macromol. Biosci.*, 2022, **22**, e2100361.

4 E. L. Krasnopeeva, G. G. Panova and A. V. Yakimansky, Agricultural Applications of Superabsorbent Polymer Hydrogels, *Int. J. Mol. Sci.*, 2022, **23**, 15134.

5 M. Hamidi, A. Azadi and P. Rafiei, Hydrogel nanoparticles in drug delivery, *Adv. Drug Delivery Rev.*, 2008, **60**, 1638–1649.

6 J. L. West and J. A. Hubbell, Photopolymerized hydrogel materials for drug delivery applications, *React. Polym.*, 1995, **25**, 139–147.

7 M. D. Markovic, V. V. Panic, S. I. Savic, V. D. Ugrinovic, R. V. Pjanovic, M. M. Spasojevic and P. M. Spasojevic, Biobased thermo/pH sensitive poly(N-isopropylacrylamide-co-crotonic acid) hydrogels for targeted drug delivery, *Microporous Mesoporous Mater.*, 2022, **335**, 111817.

8 V. Van Tran, D. Park and Y. C. Lee, Hydrogel applications for adsorption of contaminants in water and wastewater treatment, *Environ. Sci. Pollut. Res. Int.*, 2018, **25**, 24569–24599.

9 Q. Yi, J. Tan, W. Liu, H. Lu, M. Xing and J. Zhang, Peroxymonosulfate activation by three-dimensional cobalt hydroxide/graphene oxide hydrogel for wastewater treatment through an automated process, *Chem. Eng. J.*, 2020, **400**, 125965.

10 H. Huang, X. Zhang, Z. Dong, X. Zhao and B. Guo, Nanocomposite conductive tough hydrogel based on metal coordination reinforced covalent Pluronic F-127 micelle network for human motion sensing, *J. Colloid Interface Sci.*, 2022, **625**, 817–830.

11 L. Oatway, T. Vasanthan and J. H. Helm, Phytic Acid, *Food Rev. Int.*, 2007, **17**, 419–431.

12 Q. Hu, G. Li, X. Liu, B. Zhu, X. Chai, Q. Zhang, J. Liu and C. He, Superhydrophilic Phytic-Acid-Doped Conductive Hydrogels as Metal-Free and Binder-Free Electrocatalysts for Efficient Water Oxidation, *Angew. Chem., Int. Ed. Engl.*, 2019, **58**, 4318–4322.

13 Z. Wang, Z. Ma, S. Wang, M. Pi, X. Wang, M. Li, H. Lu, W. Cui and R. Ran, Cellulose nanocrystal/phytic acid reinforced conductive hydrogels for antifreezing and antibacterial wearable sensors, *Carbohydr. Polym.*, 2022, **298**, 120128.

14 C. Li, Z. Hou and P. Li, Phytic acid-assist for self-healing nanocomposite hydrogels with surface functionalization of cellulose nanocrystals via SI-AGET ATRP, *Cellulose*, 2023, **30**, 1087–1102.

15 K. Chen, S. Zhang, A. Li, X. Tang, L. Li and L. Guo, Bioinspired Interfacial Chelating-like Reinforcement Strategy toward Mechanically Enhanced Lamellar Materials, *ACS Nano*, 2018, **12**, 4269–4279.

16 K. T. Nguyen and J. L. West, Photopolymerizable hydrogels for tissue engineering applications, *Biomaterials*, 2002, **23**(22), 4307–4314.

17 C. Decker, UV-curing chemistry: past, present and future, *J. Coat. Technol.*, 1987, **59**(751), 97–106.

18 N. Zivic, M. Bouzrati-Zerrelli and S. Villotte, A novel naphthalimide scaffold based iodonium salt as a one-component photoacid/photoinitiator for cationic and radical polymerization under LED exposure, *Polym. Chem.*, 2016, **7**, 5873–5979.

19 Y. Jiang, S. Li, Y. Chen, S. Yan, M. Tao and P. Wen, Facile and Green Preparation of Superfast Responsive Macroporous Polyacrylamide Hydrogels by Frontal Polymerization of Polymerizable Deep Eutectic Monomers, *Ind. Eng. Chem. Res.*, 2020, **59**, 1526–1533.

20 Q. Zhang, K. De Oliveira Vigier, S. Royer and F. Jerome, Deep eutectic solvents: syntheses, properties and applications, *Chem. Soc. Rev.*, 2012, **41**, 7108–7146.

21 G. De Alvarenga, B. M. Hryniewicz, I. Jasper, R. J. Silva, V. Klobukoski, F. S. Costa, T. N. M. Cervantes, C. D. B. Silva and M. Vidotti, Recent trends of micro and nanostructured conducting polymers in health and environmental applications, *J. Electroanal. Chem.*, 2020, **879**, 114754.

22 D. Song, B. Kang, Z. Zhao and S. Song, Stretchable self-healing hydrogels capable of heavy metal ion scavenging, *RSC Adv.*, 2019, **9**, 19039–19047.

23 D. Han, H. Zhao, L. Gao, Z. Qin, J. Ma, Y. Han and T. Jiao, Preparation of carboxymethyl chitosan/phytic acid composite hydrogels for rapid dye adsorption in wastewater treatment, *Colloids Surf., A*, 2021, **628**, 127355.

24 T. Zhang, H. Yan, L. Shen, Z. Fang, X. Zhang, J. Wang and B. Zhang, Chitosan/Phytic Acid Polyelectrolyte Complex: A Green and Renewable Intumescent Flame Retardant System for Ethylene–Vinyl Acetate Copolymer, *Ind. Eng. Chem. Res.*, 2014, **53**, 19199–19207.

25 F. Jamali, N. Etminani-Esfahani and A. Rahmati, Maleic acid as an important monomer in synthesis of stimuli-responsive poly(acrylic acid-co-acrylamide-co-maleic acid) superabsorbent polymer, *Sci. Rep.*, 2023, **13**, 3511.

26 J. Zhang, A. Li and A. Wang, Synthesis and characterization of multifunctional poly(acrylic acid-co-acrylamide)/sodium humate superabsorbent composite, *React. Funct. Polym.*, 2006, **66**, 747–756.

27 T. Singh and R. Singhal, Poly(acrylic acid/acrylamide/sodium humate) superabsorbent hydrogels for metal ion/dye adsorption: Effect of sodium humate concentration, *J. Appl. Polym. Sci.*, 2012, **125**, 1267–1283.

28 J. Zhang, R. Liu, A. Li and A. Wang, Preparation, Swelling Behaviors, and Slow-Release Properties of a Poly(acrylic acid-co-acrylamide)/Sodium Humate Superabsorbent, *Composite*, 2005, **45**, 48–53.

29 Q. Jiang, P. Li, Y. Liu and P. Zhu, Phytic Acid-Iron/Laponite Coatings for Enhanced Flame Retardancy, Antidripping and Mechanical Properties of Flexible Polyurethane Foam, *Int. J. Mol. Sci.*, 2022, **23**, 9145.

30 Q. Yang, C. Gao, X. Zhang, C. Tsou, X. Zhao, M. R. De Guzman, Z. Pu, X. Li, Y. Lu, C. Zeng, L. Yuan, Y. Xia, Y. Sheng and Y. Fu, A Dual Physical Cross-Linking Strategy to Construct Tough Hydrogels with High Strength, Excellent Fatigue Resistance, and Stretching-Induced Strengthening Effect, *Macromol. Mater. Eng.*, 2021, **306**(7), 2100093.

31 R. a. Li, T. Fan, G. Chen, H. Xie, B. Su and M. He, Highly transparent, self-healing conductive elastomers enabled by synergistic hydrogen bonding interactions, *Chem. Eng. J.*, 2020, **393**, 124685.

32 S. Zhang, Y. Zhang, B. Li, P. Zhang, L. Kan, G. Wang, H. Wei, X. Zhang and N. Ma, One-Step Preparation of a Highly Stretchable, Conductive, and Transparent Poly(vinyl alcohol)-Phytic Acid Hydrogel for Casual Writing Circuits, *ACS Appl. Mater. Interfaces*, 2019, **11**, 32441–32448.

33 M.-Y. Zhao, Y.-D. Wang, D. Cheng, B.-L. Liu, Y.-H. Wang and H.-Y. Zang, A highly proton conductive membrane based on hydrolyzed NbCl5 and phytic acid, *Int. J. Hydrogen Energy*, 2020, **45**, 14539–14546.

34 Y. Li, Z. Li, W. Wang and J. Sun, Self-healing and highly elastic fluorine-free proton exchange membranes comprised of poly(vinyl alcohol) derivative and phytic acid for durable fuel cells, *Sci. China Mater.*, 2020, **63**, 1235–1246.

35 N. Kanmaz, D. Saloglu and J. Hizal, Humic acid embedded chitosan/poly (vinyl alcohol) pH-sensitive hydrogel: synthesis, characterization, swelling kinetic and diffusion coefficient, *Chem. Eng. Commun.*, 2018, **206**, 1168–1180.

36 M. C. Mohd Amin, N. Ahmad, M. Pandey and C. Jue Xin, Stimuli-responsive bacterial cellulose-g-poly(acrylic acid-co-acrylamide) hydrogels for oral controlled release drug delivery, *Drug Dev. Ind. Pharm.*, 2014, **40**, 1340–1349.

37 B. Işık, Swelling behavior and determination of diffusion characteristics of acrylamide-acrylic acid hydrogels, *J. Appl. Polym. Sci.*, 2004, **91**, 1289–1293.

38 G. T. Chao, Z. Y. Qian, M. J. Huang, B. Kan, Y. C. Gu, C. Y. Gong, J. L. Yang, K. Wang, M. Dai, X. Y. Li, M. L. Gou, M. J. Tu and Y. Q. Wei, Synthesis, characterization, and hydrolytic degradation behavior of a novel biodegradable pH-sensitive hydrogel based on polycaprolactone, methacrylic acid, and poly(ethylene glycol), *J. Biomed. Mater. Res., Part A*, 2008, **85**, 36–46.

39 L. J. Feng, J. X. Yuan, H. B. Lei and X. R. Zheng, Preparation of Poly Acrylic Acid Acrylamide Nanometer Material and its Drug Delivery Control Potential in Alkaline Condition, *Mater. Sci. Forum*, 2016, **873**, 84–88.